05

Transversely Diode-Pumped Metastable Rare Gas Atoms Laser Radiation Amplifier

© A.I. Parkhomenko, A.M. Shalagin

Institute of Automation and Electrometry, Siberian Branch, Russian Academy of Sciences,
630090 Novosibirsk, Russia

e-mail: par@iae.nsk.su, shalagin@iae.nsk.su

Received March 09, 2023
Revised September 28, 2023
Accepted September 28, 2023

A theoretical analysis of a radiation amplifier based on metastable noble gas atoms excited by laser diodes in transverse pumping mode is presented. In the case when the amplified radiation reaches a sufficiently high intensity, the original equations allow a simple analytical solution, from which all the most important characteristics of the amplifier and the optimal parameters of both the working environment and the pump radiation, which ensure the most efficient operation of the amplifier, are easily found.

Keywords: laser radiation amplifier, diode pumping, inert gases, metastable atoms, collisions.

DOI: 10.61011/EOS.2023.09.57346.4682-23

1. Introduction

A new type of gas lasers, diode-pumped rare gas lasers (DPRGLs), has attracted considerable research attention in the last decade [1–17]. The intense interest in these lasers stems from their theoretical capacity to produce high-power (megawatt) continuous radiation. In terms of the physical mechanism of operation, they are similar to diode-pumped alkali vapor lasers [18–21], but have an advantage in that the gas medium is chemically inert.

Excited $1s$ and $2p$ levels of Ne, Ar, Kr, and Xe atoms (ordered by energy, these are four $1s$ levels $1s_5, \ldots, 1s_2$ and ten $2p$ levels $2p_{10}, \ldots, 2p_1$) are used in DPRGLs. Metastable atoms in the lowest-energy metastable state $1s_5$ are produced by an electric discharge. A rough description of the laser operation is provided by a three-level V diagram (with only the $1s_5$, $2p_{10}$, and $2p_9$ levels taken into account) [3]. Pump diode radiation is absorbed resonantly from metastable state $1s_5$ to excited state $2p_9$. At a sufficiently high buffer gas pressure, collisional transitions between levels $2p_9$ and $2p_{10}$ result in efficient filling of level $2p_{10}$, which leads to population inversion between levels $2p_{10}$ and $1s_5$ and lasing at the $2p_{10}$–$1s_5$ transition frequency.

The first theoretical estimates of DPRGL operation efficiency have been made in [3] based on a three-level model of active particles. A five-level DPRGL model (with the $1s_5$, $1s_4$, $2p_{10}$, $2p_9$, and $2p_8$ levels taken into account) has been proposed later in [6]. Compared to the three-level model of active particles, the five-level one provides a closer approximation of the actual structure of energy levels of excited rare gas atoms and allows one to calculate the DPRGL operation parameters more accurately.

The maximum DPRGL radiation power achieved to date is 4.1 W (a continuous-wave Ar metastable laser with longitudinal diode pumping) [8]. The process needs to be scaled to achieve a significant increase in output power. The laser design most suitable for output power scaling is the one with transverse pumping, which allows one to achieve high radiation power levels by extending the length of the active medium. The theoretical output power for a DPRGL with transverse diode pumping is as high as several tens of kilowatts at an active medium length of approximately 20 cm [17].

The use of a drive oscillator power amplifier configuration is an alternative (to the use of a sole oscillator) way to scale the DPRGL power. The drive oscillator produces coherent radiation, and the optical amplifier raises the power of radiation while maintaining its desired properties. With the amplifier designed as a separate unit, one avoids unnecessary enhancement of the radiation intensity within the laser cavity and moderates the thermal effect of power lasers.

In the present study, the five-level model is used as a framework to develop an analytical method for calculation of the energy parameters of a metastable rare gas amplifier of laser radiation with transverse diode pumping.

2. Modeling the amplifier operation

Let us use the five-level model of active particles [6,7] (Fig. 1) to calculate the energy characteristics of a diode-pumped rare gas amplifier (DPRGA). For clarity, atomic levels are denoted with numbers in Fig. 1; the statistical weights of levels are also indicated: $g_1 = 5$, $g_2 = 3$, $g_3 = 3$, $g_4 = 7$, and $g_5 = 5$. Dashed and thin straight arrows correspond to the processes of spontaneous emission and collisional relaxation, respectively, while thick arrows represent pumping and lasing processes.

Let us examine the DPRGA operation with transverse diode pumping. The schematic DPRGA diagram is shown

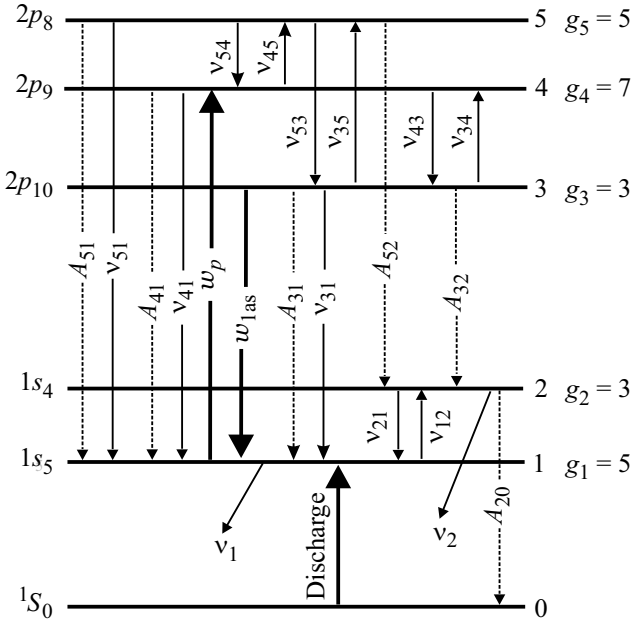

Figure 1. Diagram of working levels and transitions in rare gas atoms.

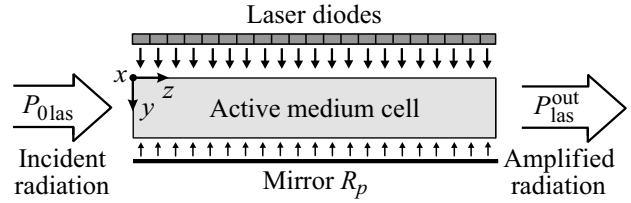

Figure 2. Diagram of a metastable rare gas amplifier of laser radiation with transverse diode pumping.

in Fig. 2. The cell is filled with metastable rare gas atoms and buffer gas. It is assumed that the cell has the shape of a rectangular parallelepiped with length z_0, width y_0, and height x_0. Pump diode radiation propagates along axis y within the cell and is reflected back to the second pass by the side mirror with reflection coefficient R_p. Amplified laser radiation propagates along axis z within the cell. It is assumed for simplicity that the intensity distribution of pump and amplified radiation at the cell inlet is uniform. It follows that the intensity distribution of amplified radiation within the cell may be considered to be uniform along axis x.

Equations characterizing the absorption of pump radiation and amplification of laser radiation are written as

$$\frac{\partial I^{\pm}_{\omega p}(y,z,\omega)}{\partial y} = \mp \left[N_1(y,z) - \frac{g_1}{g_4} N_4(y,z)\right] \times \sigma_p(\omega) I^{\pm}_{\omega p}(y,z,\omega),$$

$$\frac{\partial I_{las}(y,z)}{\partial z} = \left[N_3(y,z) - \frac{g_3}{g_1} N_1(y,z)\right] \sigma_{las}(\omega_{las}) I_{las}(y,z). \quad (1)$$

Here, $I^{+}_{\omega p}(y,z,\omega)$ and $I^{-}_{\omega p}(y,z,\omega)$ are the spectral intensity densities of pump radiation with frequency ω propagating along axis y and in the opposite direction; $I_{las}(y,z)$ is the intensity of amplified laser radiation; and $N_i(y,z)$ is the population of level i. Cross section $\sigma_p(\omega)$ of pump radiation absorption and cross section $\sigma_{las}(\omega_{las})$ of induced radiation with the emission of a photon with frequency ω_{las} are calculated as

$$\sigma_p(\omega) = \frac{g_4}{g_1}\frac{\lambda_p^2 A_{41}}{4\pi}\frac{\Gamma_p}{\Gamma_p^2 + (\omega - \omega_{41})^2},$$

$$\sigma_{las}(\omega_{las}) = \frac{\lambda_{las}^2 A_{31}}{4\pi}\frac{\Gamma_{las}}{\Gamma_{las}^2 + (\omega_{las} - \omega_{31})^2},$$

$$\Gamma_p = A_{41}/2 + \gamma_{41}, \qquad \Gamma_{las} = (A_{31} + A_{32})/2 + \gamma_{31}, \quad (2)$$

where λ_p and λ_{las} are the wavelengths of pump and amplified radiation; A_{ki} are the rates of spontaneous emission for $k - i$ transitions; ω_{31} and ω_{41} are the frequencies of transitions 3–1 and 4–1; and γ_{31} and γ_{41} are the collisional half-widths of 3–1 and 4–1 transition lines. Differential equations (1) are supplemented with three boundary conditions (at $z = 0$, $y = 0$, $y = y_0$):

$$I_{las}(y,0) = I_{0las},$$

$$I^{+}_{\omega p}(0,z,\omega) = I_{0\omega p}(\omega),$$

$$I^{-}_{\omega p}(y_0,z,\omega) = R_p I^{+}_{\omega p}(y_0,z,\omega). \quad (3)$$

Balance equations for level populations take the form

$$\frac{dN_5}{dt} = 0 = -\Gamma_5 N_5(y,z) + \nu_{45} N_4(y,z) + \nu_{35} N_3(y,z),$$

$$\frac{dN_4}{dt} = 0 = w_p(y,z)\left[N_1(y,z) - \frac{g_1}{g_4} N_4(y,z)\right] - \Gamma_4 N_4(y,z) + \nu_{54} N_5(y,z) + \nu_{34} N_3(y,z),$$

$$\frac{dN_3}{dt} = 0 = -w_{las}(y,z)\left[N_3(y,z) - \frac{g_3}{g_1} N_1(y,z)\right] - \Gamma_3 N_3(y,z) + \nu_{43} N_4(y,z) + \nu_{53} N_5(y,z),$$

$$\frac{dN_2}{dt} = 0 = -\Gamma_2 N_2(y,z) + A_{52} N_5(y,z) + A_{32} N_3(y,z) + \nu_{12} N_1(y,z),$$

$$N_1(y,z) + N_2(y,z) + N_3(y,z) + N_4(y,z) + N_5(y,z) = N, \quad (4)$$

where the following notation is introduced:

$$\Gamma_2 = A_{20} + \nu_{21} + \nu_2,$$

$$\Gamma_3 = A_{31} + A_{32} + \nu_{31} + \nu_{34} + \nu_{35},$$

$$\Gamma_4 = A_{41} + \nu_{41} + \nu_{43} + \nu_{45},$$

$$\Gamma_5 = A_{51} + A_{52} + \nu_{51} + \nu_{53} + \nu_{54}. \quad (5)$$

Here, ν_{ki} are the frequencies of inelastic collisional transitions between levels in channels $k \to i$; ν_2 is the loss frequency for level 2 (due to excimer formation); Γ_i ($i = 2, 3, 4, 5$) is the overall loss frequency for level i (due to spontaneous emission and collisions); and N is the overall concentration of active atoms at all five levels (set as a constant). Probabilities $w_{\text{las}}(y, z)$ and $w_p(y, z)$ of induced transitions under the influence of amplified laser radiation and pump radiation are determined using the following formulae:

$$w_{\text{las}}(y, z) = \frac{\sigma_{\text{las}}(\omega_{\text{las}})}{\hbar\omega_{\text{las}}} I_{\text{las}}(y, z),$$

$$w_p(y, z) = \int_0^\infty \frac{\sigma_p(\omega)}{\hbar\omega_p} I_{\omega p}(y, z, \omega)\, d\omega,$$

$$I_{\omega p}(y, z, \omega) = I^+_{\omega p}(y, z, \omega) + I^-_{\omega p}(y, z, \omega), \qquad (6)$$

where ω_p is the center frequency of broadband pump radiation and $I_{\omega p}(y, z, \omega)$ is the overall spectral intensity density of pump radiation within the cell. In accordance with the principle of detailed balance, frequencies ν_{ki} and ν_{ik} of direct and reverse collisional transitions between levels k and i are related as

$$\nu_{ik} = \nu_{ki} \frac{g_k}{g_i} \exp\left(-\frac{E_k - E_i}{k_B T}\right), \qquad (7)$$

where E_k and E_i are the energies of upper (k) and lower (i) levels, k_B is the Boltzmann constant, and T is temperature.

Population differences, which are found in differential equations (1) and govern the absorption of pump radiation and amplification of laser radiation, are derived from system (4):

$$N_1(y, z) - \frac{g_1}{g_4} N_4(y, z) = N \frac{q\varkappa_{\text{las}} + \delta}{1 + \varkappa_p + \varkappa_{\text{las}} + b\varkappa_p\varkappa_{\text{las}}},$$

$$N_3(y, z) - \frac{g_3}{g_1} N_1(y, z) = N \frac{a\varkappa_p - \alpha_2\delta}{1 + \varkappa_p + \varkappa_{\text{las}} + b\varkappa_p\varkappa_{\text{las}}}, \qquad (8)$$

where

$$a = \frac{\Gamma_2}{K_1}[\Gamma_5(\nu_{43} - \alpha_1\alpha_2\Gamma_3) + \nu_{53}(\nu_{45} + \alpha_1\alpha_2\nu_{35})],$$

$$q = \frac{\Gamma_2}{K_2}[\Gamma_5(\Gamma_4 - \alpha_1\alpha_2\nu_{34}) - \nu_{54}(\nu_{45} + \alpha_1\alpha_2\nu_{35})],$$

$$\delta = \frac{\Gamma_2}{\Gamma_2 + \nu_{12}}, \quad b = \frac{K_0 K_3}{K_1 K_2}, \quad \alpha_1 = \frac{g_1}{g_4}, \quad \alpha_2 = \frac{g_3}{g_1},$$

$$K_0 = (\Gamma_2 + \nu_{12})[\Gamma_5(\Gamma_3\Gamma_4 - \nu_{34}\nu_{43}) - \nu_{35}(\Gamma_4\nu_{53} + \nu_{43}\nu_{54}) - \nu_{45}(\Gamma_3\nu_{54} + \nu_{34}\nu_{53})],$$

$$K_1 = \Gamma_5\{\Gamma_2[(1 + \alpha_1)\Gamma_3 + \nu_{43}] + \alpha_1\nu_{12}\Gamma_3 + \nu_{43}A_{32}\} + \nu_{45}[\Gamma_2(\Gamma_3 + \nu_{53}) + \nu_{53}A_{32} + \Gamma_3 A_{52}] + \nu_{35}\{\Gamma_2[\nu_{43} - (1 + \alpha_1)\nu_{53}] + \nu_{43}A_{52} - \alpha_1\nu_{12}\nu_{53}\},$$

$$K_2 = \Gamma_5\{\Gamma_4[(1 + \alpha_2)\Gamma_2 + \alpha_2 A_{32} + \nu_{12}] + \alpha_2\nu_{34}\Gamma_2\} + \nu_{45}\{\alpha_2\nu_{34}(\Gamma_2 + A_{52}) - \nu_{54}[\nu_{12} + (1 + \alpha_2)\Gamma_2 + \alpha_2 A_{32}]\} + \alpha_2\nu_{35}[\Gamma_4(\Gamma_2 + A_{52}) + \nu_{54}\Gamma_2],$$

$$K_3 = \Gamma_5[(1 + \alpha_1 + \alpha_1\alpha_2)\Gamma_2 + \alpha_1(\nu_{12} + \alpha_2 A_{32})]. \qquad (9)$$

Dimensionless quantities $\varkappa_p \equiv \varkappa_p(y, z)$ and $\varkappa_{\text{las}} \equiv \varkappa_{\text{las}}(y, z)$, which are given by

$$\varkappa_p = \frac{w_p(y, z)}{\beta_p}, \quad \varkappa_{\text{las}} = \frac{w_{\text{las}}(y, z)}{\beta_{\text{las}}}, \quad \beta_p = \frac{K_0}{K_1}, \quad \beta_{\text{las}} = \frac{K_0}{K_2}, \qquad (10)$$

have the meaning of saturation parameters: they characterize the degree of equalization of population at transitions 4–1 and 3–1 when there is no second field.

The following final form of differential equations (1), which characterize the operation of the laser radiation amplifier, is obtained with the use of formulae (8):

$$\frac{\partial I^\pm_{\omega p}(y, z, \omega)}{\partial y} = \mp \frac{(q\varkappa_{\text{las}} + \delta) N \sigma_p(\omega) I^\pm_{\omega p}(y, z, \omega)}{1 + \varkappa_p + \varkappa_{\text{las}} + b\varkappa_p\varkappa_{\text{las}}},$$

$$\frac{\partial I_{\text{las}}(y, z)}{\partial z} = \frac{(a\varkappa_p - \alpha_2\delta) N \sigma_{\text{las}}(\omega_{\text{las}}) I_{\text{las}}(y, z)}{1 + \varkappa_p + \varkappa_{\text{las}} + b\varkappa_p\varkappa_{\text{las}}}. \qquad (11)$$

It follows from the last equation in (11) that radiation amplification is feasible only when condition $a\varkappa_p > \alpha_2\delta$ is satisfied. Efficient operation of the amplifier requires fulfillment of condition $a\varkappa_p \gg \alpha_2\delta$, which may be presented in the form of two conditions:

$$\nu_{43} \gg A_{31} + A_{32} + \nu_{31}, \quad \varkappa_p \gg 1. \qquad (12)$$

The first condition in (12) is satisfied under a sufficiently high buffer gas pressure (several hundred torr and above) and implies that, owing to frequent collisional transitions between excited levels 4 and 3, an equilibrium Boltzmann population distribution sets in within a time interval shorter than the lifetime of these levels. The second condition in (12) is satisfied at a sufficiently high spectral intensity density of pump radiation.

3. Analytical solution of the problem in the case of a high intensity of amplified radiation

In its general form, the system of differential equations (11) does not have an analytical solution and may be solved only numerically. However, if the intensity of amplified radiation is so high that conditions

$$\varkappa_{\text{las}} \gg \frac{1 + \varkappa_p}{1 + b\varkappa_p}, \frac{\delta}{q}, \qquad b\varkappa_p \lesssim 1 \qquad (13)$$

are satisfied, Eqs. (11) may be simplified considerably and have rather a simple analytical solution. In the working medium of the amplifier, the value of δ/q is normally several times greater than unity (for example, $\delta/q = 2$–3

for metastable Ar atoms in buffer He gas). Since efficient amplifier operation is established at $\varkappa_p \gg 1$, the first condition in (13) is effectively the same as $\varkappa_{las} \gg \varkappa_p$. Under conditions (12) of efficient amplifier operation, coefficient b is always well below unity (in order of magnitude, $b \sim (A_{31} + A_{32} + \nu_{31})/\nu_{43} \ll 1$). Owing to the smallness of coefficient b, we assume that $b\varkappa_p$ is bounded from above by condition $b\varkappa_p \lesssim 1$.

Under conditions (13), the system of differential equations (11) is simplified greatly and takes the form

$$\frac{\partial I^{\pm}_{\omega p}(y,\omega)}{\partial y} = \mp qN\sigma_p(\omega)\frac{I^{\pm}_{\omega p}(y,\omega)}{1+b\varkappa_p(y)},$$

$$\frac{\partial I_{las}(y,z)}{\partial z} = N\beta_{las}\hbar\omega_{las}\frac{a\varkappa_p(y)-\alpha_2\delta}{1+b\varkappa_p(y)}, \qquad (14)$$

where saturation parameter $\varkappa_p$ is given by

$$\varkappa_p(y) = \frac{1}{\beta_p\hbar\omega_p}\int_0^\infty \sigma_p(\omega)\left[I^{+}_{\omega p}(y,\omega) + I^{-}_{\omega p}(y,\omega)\right]d\omega. \qquad (15)$$

The solution of the last equation in (14) for the intensity of amplified radiation, which satisfies boundary conditions (3), is simple in form:

$$I_{las}(y,z) = I_{0las} + Nz\beta_{las}\hbar\omega_{las}\frac{a\varkappa_p(y)-\alpha_2\delta}{1+b\varkappa_p(y)}. \qquad (16)$$

It is evident that the intensity of amplified radiation within the cell depends linearly on z under conditions (13). This dependence suggests that the population inversion in the active medium is suppressed almost completely when a high-power signal is passed through the amplifier.

Intensity $I^{out}_{las}(y)$ of output laser radiation is defined by $I^{out}_{las}(y) = I_{las}(y, z_0)$ and written as

$$I^{out}_{las}(y) = I_{0las} + Nz_0\beta_{las}\hbar\omega_{las}\frac{a\varkappa_p(y)-\alpha_2\delta}{1+b\varkappa_p(y)}. \qquad (17)$$

A linear dependence of the output radiation intensity on cell length z_0 is evident. Total output laser radiation power P^{out}_{las} is determined as an integral of intensity over the cross section of the cell:

$$P^{out}_{las} = x_0\int_0^{y_0} I^{out}_{las}(y)\,dy = $$

$$= P_{0las} + Nx_0z_0\beta_{las}\hbar\omega_{las}\int_0^{y_0}\frac{a\varkappa_p(y)-\alpha_2\delta}{1+b\varkappa_p(y)}\,dy, \qquad (18)$$

where $P_{0las} = x_0y_0I_{0las}$ is the input laser radiation power.

Saturation parameter $\varkappa_p(y)$, which is found in expressions (16)–(18), may be determined using the first two equations for $I^{\pm}_{\omega p}(y,\omega)$ in (14). Let us solve the system of two differential equations by the method of successive approximations with respect to small parameter $b\varkappa_p$. In the zeroth-order approximation (at $b = 0$), the first two equations in (14) take the form

$$\frac{\partial I^{\pm(0)}_{\omega p}(y,\omega)}{\partial y} = \mp qN\sigma_p(\omega)I^{\pm(0)}_{\omega p}(y,\omega). \qquad (19)$$

The solution of these equations satisfying boundary conditions (3) is given by

$$I^{+(0)}_{\omega p}(y,\omega) = I_{0\omega p}(\omega)\exp\left[-q\sigma_p(\omega)Ny\right],$$

$$I^{-(0)}_{\omega p}(y,\omega) = R_p\,I_{0\omega p}(\omega)\exp\left[-q\sigma_p(\omega)N(2y_0-y)\right]. \qquad (20)$$

In the next approximation, the first two equations in (14) take the form

$$\frac{\partial I^{\pm(1)}_{\omega p}(y,\omega)}{\partial y} = \mp\frac{qN\sigma_p(\omega)I^{\pm(1)}_{\omega p}(y,\omega)}{1+b\varkappa^{(0)}_p(y)}, \qquad (21)$$

where the initial approximate value of saturation parameter $\varkappa^{(0)}_p$ is specified by formula (15) with $I^{\pm}_{\omega p}(y,\omega)$ substituted by $I^{\pm(0)}_{\omega p}(y,\omega)$. The solution of Eqs. (21) satisfying boundary conditions (3) is given by

$$I^{+(1)}_{\omega p}(y,\omega) = I_{0\omega p}(\omega)\exp\left\{-qN\sigma_p(\omega)\varphi(y)\right\},$$

$$I^{-(1)}_{\omega p}(y,\omega) = R_p\,I_{0\omega p}(\omega)\exp\left\{qN\sigma_p(\omega)\left[\varphi(y)-2\varphi(y_0)\right]\right\},$$

$$\varphi(y) = \int_0^y\frac{dy}{1+b\varkappa^{(0)}_p(y)}. \qquad (22)$$

The resulting expression for saturation parameter $\varkappa_p$ is

$$\varkappa_p(y) \equiv \varkappa^{(1)}_p(y) = \frac{1}{\beta_p\hbar\omega_p}\int_0^\infty\sigma_p(\omega)$$

$$\times\left[I^{+(1)}_{\omega p}(y,\omega) + I^{-(1)}_{\omega p}(y,\omega)\right]d\omega, \qquad (23)$$

where the spectral intensity densities of pump radiation are specified by relations (22).

4. Analysis of amplifier operation

A spectral intensity density of input radiation of pump diodes needs to be set in order to calculate specific energy characteristics of the amplifier with the use of the above formulae. Let us assume that the pump spectrum at the cell inlet is Gaussian

$$I_{0\omega p}(\omega) = \frac{I_{0p}}{\sqrt{\pi}\Delta\omega}\exp\left[-\left(\frac{\omega-\omega_p}{\Delta\omega}\right)^2\right] \qquad (24)$$

with half-width $\Delta\omega$ (at height $1/e$); I_{0p} is the overall intensity of input radiation of pump diodes.

The following expression for the overall spectral intensity density of pump radiation within the

cell, which is defined as $I_{\omega p}(y,\omega) = I_{\omega p}^{+(1)}(y,\omega) + +I_{\omega p}^{-(1)}(y,\omega)$, is derived from relations (22) and (24):

$$I_{\omega p}(y,\omega) = \frac{I_{0p}}{\sqrt{\pi}\Delta\omega}\{\exp[-g(\omega,y)] + R_p\exp[g(\omega,y) - 2g(\omega,y_0)]\},$$

$$g(\omega,y) = \left(\frac{\omega-\omega_p}{\Delta\omega}\right)^2 + qN\sigma_p(\omega)\varphi(y). \qquad (25)$$

The relation for saturation parameter $\varkappa_p^{(0)}(y)$ found in the formula for function $\varphi(y)$ in (22) is

$$\varkappa_p^{(0)}(y) = \frac{\sigma_p(\omega_{41})I_{0p}}{\beta_p\hbar\omega_p}[f_2(y) + R_p f_2(2y_0 - y)],$$

$$f_2(y) = \frac{1}{\sqrt{\pi}\Delta\omega}\int_0^\infty \frac{\exp[-g_0(\omega,y)]}{1+[(\omega-\omega_{41})/\Gamma_p]^2}\,d\omega,$$

$$g_0(\omega,y) = \left(\frac{\omega-\omega_p}{\Delta\omega}\right)^2 + q\sigma_p(\omega)Ny. \qquad (26)$$

Overall pump radiation intensity $I_p(y) = \int_0^\infty I_{\omega p}(y,\omega)\,d\omega$ within the cell is determined using (25):

$$I_p(y) = \frac{I_{0p}}{\sqrt{\pi}\Delta\omega}\int_0^\infty \{\exp[-g(\omega,y)] + R_p\exp[g(\omega,y) - 2g(\omega,y_0)]\}d\omega. \qquad (27)$$

Under such conditions, saturation parameter $\varkappa_p(y)$ is given by

$$\varkappa_p(y) = \frac{\sigma_p(\omega_{41})I_{0p}}{\sqrt{\pi}\Delta\omega\beta_p\hbar\omega_p} \times \int_0^\infty \frac{\exp[-g(\omega,y)] + R_p\exp[g(\omega,y) - 2g(\omega,y_0)]}{1+[(\omega-\omega_{41})/\Gamma_p]^2}\,d\omega. \qquad (28)$$

Using (18), we find the ratio of radiation power increment $P_{\text{las}}^{\text{inc}} = P_{\text{las}}^{\text{out}} - P_{0\text{las}}$ in the amplifier to pump radiation power $P_{0p} = x_0 z_0 I_{0p}$ (this ratio characterizes the efficiency of conversion of pump radiation into laser radiation):

$$\frac{P_{\text{las}}^{\text{inc}}}{P_{0p}} = \frac{N\beta_{\text{las}}\hbar\omega_{\text{las}}}{I_{0p}}\int_0^{y_0}\frac{a\varkappa_p(y) - \alpha_2\delta}{1+b\varkappa_p(y)}\,dy. \qquad (29)$$

Let us perform actual calculations of energy parameters of the radiation amplifier. It is assumed that metastable argon atoms form the active medium in the amplifier and helium is the buffer gas. This gas is needed for efficient collisional mixing between levels 4 and 3 in active atoms and to increase the line width of transition 4–1 with the purpose of maximizing the efficiency of utilization of broadband pump radiation.

Let us specify the initial data for numerical calculations of amplifier parameters. According to NIST data [22], Ar atoms have transition wavelengths $\lambda_{31} = 912.3$ nm and $\lambda_{41} = 811.5$ nm; level energy differences $\Delta E_{21} = 606.8\,\text{cm}^{-1}$, $\Delta E_{43} = 1360.7\,\text{cm}^{-1}$, ΔE_{53}=1515.2 cm^{-1}, and ΔE_{54}=154.5 cm^{-1}; and spontaneous emission rates A_{31}=1.89 · 10^7 s^{-1}, A_{32}=5.4 · 10^6 s^{-1}, A_{41}=3.3 · 10^7 s^{-1}, A_{51}=9.3 · 10^6 s^{-1}, A_{52}=2.15 · 10^7 s^{-1}, and A_{20}=1.32 · 10^8 s^{-1}. Radiation trapping at transition $2-0$ ($1s_4 - {}^1S_0$) occurs due to the fact that the concentration of Ar atoms in the active medium normally exceeds $10^{17}\,\text{cm}^{-3}$. The effect of radiation trapping is taken into account by introducing an effective probability of radiative transition $2 \to 0$, which is assumed to be characterized by $A_{20} = 5.7 \cdot 10^5\,\text{s}^{-1}$ [6,12,23].

The collisional broadening coefficients (half-width at half-maximum) of 3–1 and 4–1 transition lines for Ar in Ar and He are as follows [3,24,25]: $\gamma_{31}^{\text{Ar-Ar}} = 4.8$ MHz/Torr, $\gamma_{31}^{\text{Ar-He}} = 8.5$ MHz/Torr, $\gamma_{41}^{\text{Ar-Ar}}$=8.7 MHz/Torr, $\gamma_{41}^{\text{Ar-He}} =$ = 10.9 MHz/Torr.

The following expression was used to determine collision frequencies ν_{ki} that characterize inelastic collisional transitions between levels in channels $k \to i$:

$$\nu_{ki} = k_{ki}^{\text{Ar}}N_{\text{Ar}} + k_{ki}^{\text{He}}N_{\text{He}},$$

where N_{Ar} and N_{He} are the concentrations of Ar and He atoms and k_{ki}^{Ar} and k_{ki}^{He} are the rate constants of collisional transitions in channels $k \to i$ upon collisions of active particles with Ar and He atoms, respectively. The rate constants of collisional transitions at temperature $T = 300$ K are [6,12]

$k_{21}^{\text{Ar}} = 1 \cdot 10^{-13}\,\text{cm}^3/\text{s}$, $k_{21}^{\text{He}} = 1.2 \cdot 10^{-13}\,\text{cm}^3/\text{s}$,
$k_{31}^{\text{Ar}} = 6 \cdot 10^{-12}\,\text{cm}^3/\text{s}$, $k_{31}^{\text{He}} = 5 \cdot 10^{-14}\,\text{cm}^3/\text{s}$,
$k_{41}^{\text{Ar}} = 2.5 \cdot 10^{-11}\,\text{cm}^3/\text{s}$, $k_{41}^{\text{He}} = 2 \cdot 10^{-12}\,\text{cm}^3/\text{s}$,
$k_{51}^{\text{Ar}} = 1.5 \cdot 10^{-11}\,\text{cm}^3/\text{s}$, $k_{51}^{\text{He}} = 1 \cdot 10^{-12}\,\text{cm}^3/\text{s}$,
$k_{43}^{\text{Ar}} = 2.6 \cdot 10^{-11}\,\text{cm}^3/\text{s}$, $k_{43}^{\text{He}} = 1.6 \cdot 10^{-11}\,\text{cm}^3/\text{s}$,
$k_{53}^{\text{Ar}} = 1.1 \cdot 10^{-11}\,\text{cm}^3/\text{s}$, $k_{53}^{\text{He}} = 4 \cdot 10^{-12}\,\text{cm}^3/\text{s}$,
$k_{54}^{\text{Ar}} = 1.1 \cdot 10^{-11}\,\text{cm}^3/\text{s}$, $k_{54}^{\text{He}} = 4.5 \cdot 10^{-11}\,\text{cm}^3/\text{s}$.

Frequency ν_2 of loss due to excimer formation for level 2 was determined using the formula

$$\nu_2 = k_2^{\text{He}}N_{\text{Ar}}N_{\text{He}} + k_2^{\text{Ar}}N_{\text{Ar}}^2$$

with the following rate constants of excimer production at temperature $T = 300$ K [26]: $k_2^{\text{He}} = 0.48 \cdot 10^{-32}$ cm^6/s, $k_2^{\text{Ar}} = 0.95 \cdot 10^{-32}$ cm^6/s.

In what follows, the amplifier characteristics are calculated under the assumption that the frequencies of pump and amplified radiation match the frequencies of transitions 4–1 and 3–1: $\omega_p = \omega_{41}$, $\omega_{\text{las}} = \omega_{31}$.

Figure 3 presents the dependences of ratio $P_{\text{las}}^{\text{inc}}/P_{0p}$ between the radiation power increment in the amplifier and the pump radiation power on helium buffer gas pressure p_{He} at various half-widths $\Delta\omega$ of the pump radiation spectrum. Argon gas pressure p_{Ar} was set to 20 Torr. The optimum value of parameter Ny_0 (number of active atoms in a gas column with a unit cross section and height

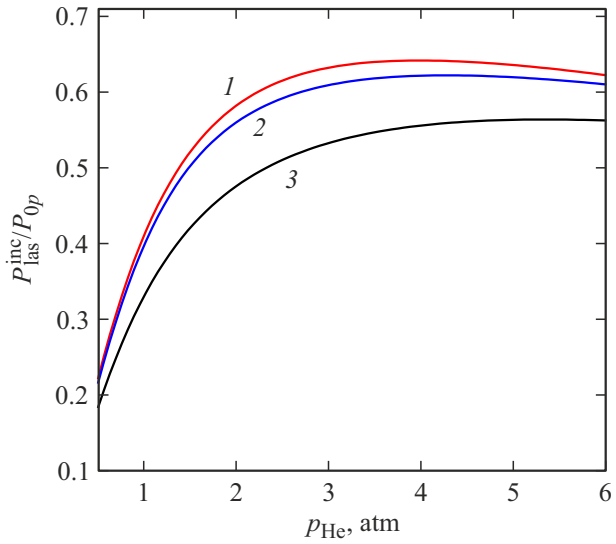

Figure 3. Dependences of efficiency P_{las}^{inc}/P_{0p} of conversion of pump radiation into laser radiation on helium buffer gas pressure p_{He} at the optimum values of parameter Ny_0, $T = 300$ K, $I_{0p} = 1$ kW/cm^2, $I_{0las} = 1$ kW/cm^2, $p_{Ar} = 20$ Torr, R_p=1 and various half-widths of the pump radiation spectrum: $\Delta\omega/(2\pi c)$=0.5 cm^{-1}, Ny_0=3.9 · 10^{13} cm^{-2} (*1*); $\Delta\omega/(2\pi c)$=1 cm^{-1}, Ny_0=4.4 · 10^{13} cm^{-2} (*2*); $\Delta\omega/(2\pi c)$=2 cm^{-1}, Ny_0=5.3 · 10^{13} cm^{-2} (*3*).

y_0) corresponding to the greatest maximum value of ratio P_{las}^{inc}/P_{0p} as a function of p_{He} was set in calculation of each curve in Fig. 3. Conditions (13) of applicability of the obtained analytical formulae are satisfied when the parameter values from Fig. 3 are used. It follows from Fig 3 that as half-width $\Delta\omega$ of the pump radiation spectrum rises, the optimum value of parameter Ny_0 increases monotonically, while efficiency P_{las}^{inc}/P_{0p} of conversion of pump radiation into laser radiation decreases monotonically: at $\Delta\omega/(2\pi c) = 0.5$ cm^{-1}, the maximum of the P_{las}^{inc}/P_{0p} ratio is 0.64 at $p_{He} = 3.9$ atm and $Ny_0 = 3.9 \cdot 10^{13}$ cm^{-2} (curve *1*), while the maximum of the P_{las}^{inc}/P_{0p} ratio for $\Delta\omega/(2\pi c) = 2$ cm^{-1} is 0.56 at $p_{He} = 5.3$ atm and $Ny_0 = 5.3 \cdot 10^{13}$ cm^{-2} (curve *3*). Note that concentration N_{1s_5} of atoms at metastable level $1s_5$ under the considered helium buffer gas pressures (p_{He} = 0.5–6 atm) and without pumping is close in magnitude to overall concentration N of active atoms at all five levels: $N_{1s_5} \approx N$.

Figure 4 illustrates the influence of parameter Ny_0 on efficiency P_{las}^{inc}/P_{0p} of conversion of pump radiation into laser radiation. Curve *1* corresponds to the optimum value of parameter Ny_0. It is evident that the conversion efficiency decreases markedly when the value of parameter Ny_0 goes above (curve *2*) or below (curve *3*) the optimum level.

The influence of input radiation intensity I_{0p} of pump diodes on the conversion efficiency is illustrated by Fig. 5. It can be seen that the conversion efficiency increases with I_{0p}: while the maximum value of ratio P_{las}^{inc}/P_{0p} at $I_{0p} = 0.3$ kW/cm^2 is 0.49 (curve *3*), the P_{las}^{inc}/P_{0p} ratio maximum at $I_{0p} = 1$ kW/cm^2 is as high as 0.62 (curve *1*). The optimum value of parameter Ny_0 also increases with I_{0p}: the optimum values of Ny_0 at input radiation intensities of 0.3 kW/cm^2 and 1 kW/cm^2 are 2.5 · 10^{13} cm^{-2} and 4.4 · 10^{13} cm^{-2}, respectively.

The side mirror, which reflects pump radiation transmitted through the cell back into it, raises the efficiency of

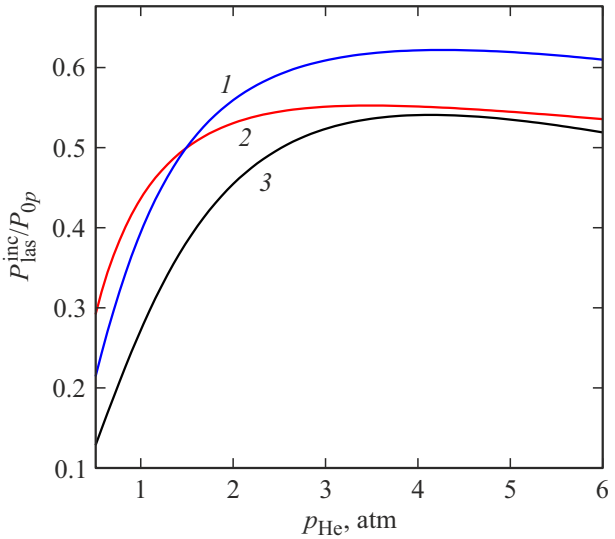

Figure 4. Dependences of efficiency P_{las}^{inc}/P_{0p} of conversion of pump radiation into laser radiation on helium buffer gas pressure p_{He} at $T = 300$ K, $I_{0p} = 1$ kW/cm^2, $\Delta\omega/(2\pi c) = 1$ cm^{-1}, $I_{0las} = 1$ kW/cm^2, $p_{Ar} = 20$ Torr, $R_p = 1$ and $Ny_0 = 4.4 \cdot 10^{13}$ (*1*), $8.8 \cdot 10^{13}$ (*2*) and $2.2 \cdot 10^{13}$ cm^{-2} (*3*).

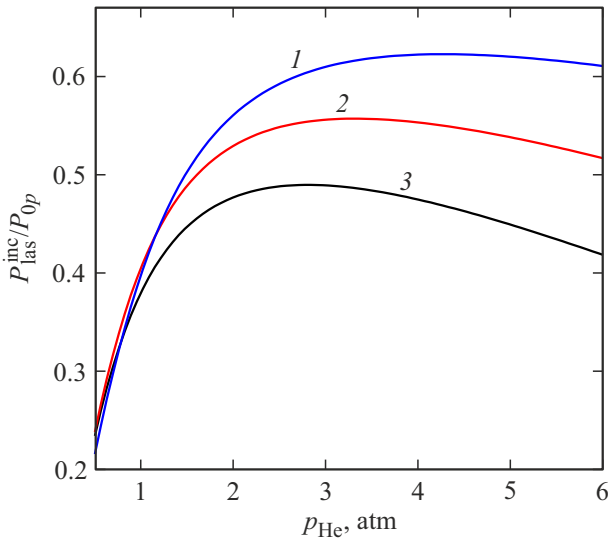

Figure 5. Dependences of conversion efficiency P_{las}^{inc}/P_{0p} on helium buffer gas pressure p_{He} at the optimum values of parameter Ny_0, $T = 300$ K, $p_{Ar} = 20$ Torr, $\Delta\omega/(2\pi c) = 1$ cm^{-1}, $R_p = 1$, and various intensities of pump radiation: $I_{0p} = 1$ kW/cm^2, $Ny_0 = 4.4 \cdot 10^{13}$ cm^{-2} (*1*); $I_{0p} = 0.5$ kW/cm^2, $Ny_0 = 3.2 \cdot 10^{13}$ cm^{-2} (*2*); $I_{0p} = 0.3$ kW/cm^2, $Ny_0 = 2.5 \cdot 10^{13}$ cm^{-2} (*3*).

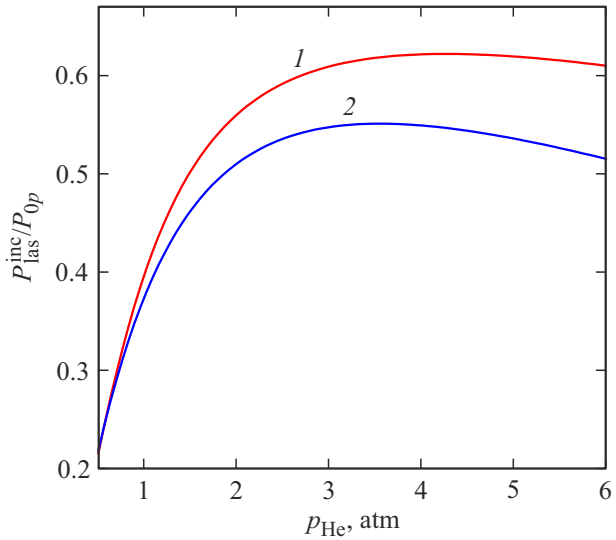

Figure 6. Dependences of conversion efficiency P_{las}^{inc}/P_{0p} on helium buffer gas pressure p_{He} at the optimum values of parameter Ny_0, $T = 300$ K, $I_{0p} = 1\,\text{kW/cm}^2$, $\Delta\omega/(2\pi c) = 1\,\text{cm}^{-1}$, $I_{0las} = 1\,\text{kW/cm}^2$, $p_{Ar} = 20\,\text{Torr}$, and various reflection coefficients R_p of the mirror: $R_p = 1$, $Ny_0 = 4.4 \cdot 10^{13}\,\text{cm}^{-2}$ (*1*); $R_p = 0$, $Ny_0 = 6.3 \cdot 10^{13}\,\text{cm}^{-2}$ (*2*).

amplifier operation. This is illustrated by Fig. 6. It follows from this figure that the maxima of ratio P_{las}^{inc}/P_{0p} in the amplifier with ($R_p = 1$) and without ($R_p = 0$) the mirror are 0.62 (curve *1*) and 0.55 (curve *2*), respectively. In addition, the conversion efficiency in the amplifier with the mirror reaches its maximum at a lower value of parameter Ny_0.

5. Conclusion

A radiation amplifier based on metastable rare gas atoms excited by laser diodes in the transverse pumping mode was analyzed theoretically. The five-level model of atoms of the active medium was taken as a basis. In the general case, the amplifier operation is characterized by a system of differential equations that may be solved only numerically. However, if the intensity of amplified radiation is sufficiently high, the original equations admit a simple analytical solution, which allows one to determine easily all of the most important amplifier characteristics and the optimum parameters of both the working medium and pump radiation.

The obtained analytical expressions suggest that ratio P_{las}^{inc}/P_{0p} between the radiation power increment in the amplifier and the pump radiation power (an indicator of amplifier efficiency) increases with increasing pump radiation intensity I_{0p} and decreasing width of the pump spectrum. Specifically, the conversion efficiency is as high as 64% at pump spectrum half-width $\Delta\omega/(2\pi c) = 0.5\ \text{cm}^{-1}$ and pump radiation intensity $I_{0p} = 1\ \text{kW/cm}^2$. An optimum value of parameter Ny_0, which characterizes the number of active atoms in a gas column with a unit cross section and height y_0, also needs to be maintained. The mirror reflecting pump radiation transmitted through the cell back into it contributes to an increase in the amplifier efficiency, ensuring that pump radiation is utilized to the fullest.

Funding

This study was funded under the state assignment (project No. AAAA-A21-121021800168-4) and was carried out at the Institute of Automation and Electrometry of the Siberian Branch of the Russian Academy of Sciences.

Conflict of interest

The authors declare that they have no conflict of interest.

References

[1] J. Han, M.C. Heaven. Opt. Lett., **37** (11), 2157 (2012). DOI: 10.1364/OL.37.002157
[2] J. Han, L. Glebov, G. Venus, M.C. Heaven. Opt. Lett., **38** (24), 5458 (2013). DOI: 10.1364/OL.38.005458
[3] A.V. Demyanov, I.V. Kochetov, P.A. Mikheyev. J. Phys. D., **46** (37), 375202 (2013). DOI: 10.1088/0022-3727/46/37/375202
[4] P.A. Mikheyev. Quantum Electron., **45** (8), 704 (2015). DOI: 10.1070/QE2015v045n08ABEH015750.
[5] W.T. Rawlins, K.L. Galbally-Kinney, S.J. Davis, A.R. Hoskinson, J.A. Hopwood, M.C. Heaven. Opt. Express, **23** (4), 4804 (2015). DOI: 10.1364/OE.23.004804
[6] Z. Yang, G. Yu, H. Wang, Q. Lu, X. Xu. Opt. Express, **23** (11), 13823 (2015). DOI: 10.1364/OE.23.013823
[7] J. Gao, Y. He , P. Sun, Z. Zhang, X. Wang, D. Zuo. Opt. Soc. Am. B, **34** (4), 814 (2017). DOI: 10.1364/JOSAB.34.000814
[8] J. Han, M.C. Heaven, P.J. Moran, G.A. Pitz, E.M. Guild, C.R. Sanderson, B. Hokr. Opt. Lett., **42** (22), 4627 (2017). DOI: 10.1364/OL.42.004627
[9] J. Gao, P. Sun, X. Wang, D. Zuo. Laser Phys. Lett., **14** (3), 035001 (2017). DOI: 10.1088/1612-202X/aa5b10
[10] A.V. Demyanov, I.V. Kochetov, P.A. Mikheyev, V.N. Azyazov, M.C. Heaven. J. Phys. D, **51** (4), 045201 (2018). DOI: 10.1088/1361-6463/aa9e40
[11] P.A. Mikheyev, A.K. Chernyshov, M.I. Svistun, N.I. Ufimtsev, O.S. Kartamysheva, M.C. Heaven, V.N. Azyazov. Opt. Express, **27** (26), 38759 (2019). DOI: 10.1364/OE.383276
[12] S. Long, Y. Qin, H. Chen, X. Wu, M. Li, X. Tang, T. Wen. Opt. Express, **27** (3), 2771 (2019). DOI: 10.1364/OE.27.002771
[13] H. Chen, S. Long, X. Tang, X. Wu, W. Wang, Y. Qin. Opt. Express, **27** (9), 12504 (2019). DOI: 10.1364/OE.27.012504
[14] P. Sun, D. Zuo, X. Wang, J. Han, M.C. Heaven. Opt. Express, **28** (10), 14580 (2020). DOI: 10.1364/OE.392810
[15] R. Wang, Z. Yang, K. Li, H. Wang, X. Xu. J. Appl. Phys., **131** (2), 023104 (2022). DOI: 10.1063/5.0079512
[16] A.A. Adamenkov, Yu.A. Adamenkov, M.V. Volkov, B.A. Vyskubenko, S.G. Garanin, M.A. Gorbunov, A.P. Domazhirov, M.V. Egorushin, A.A. Kalacheva, Yu.V. Kolobyanin, N.A. Konkina, A.A. Khlebnikov, V.A. Shaidulina, F.A. Starikov. Kvantovaya Elektron., **52** (8), 695 (2022) (in Russian).

[17] A.I. Parkhomenko, A.M. Shalagin. Kvantovaya Elektron., **52** (10), 869 (2022) (in Russian).
[18] F.W. Krupke. Progr. Quant. Electron., **36** (1), 4 (2012). DOI: 10.1016/j.pquantelec.2011.09.001
[19] A.M. Shalagin. Physics-Uspekhi, **54** (9), 975 (2011). DOI: 10.3367/UFNe.0181.201109l.1011.
[20] A.V. Bogachev, S.G. Garanin, A.M. Dudov, V.A. Eroshenko, S.M. Kulikov, G.T. Mikaelian, V.A. Panarin, V.O. Pautov, A.V. Rus, S.A. Sukharev. Quantum Electron., **42** (2), 95 (2012). DOI: 10.1070/QE2012v042n02ABEH014734.
[21] F. Gao, F. Chen, J.J. Xie, D.J. Li, L.M. Zhang, G.L. Yang, J. Guo, L.H. Guo. Optik, **124** (20), 4353 (2013). DOI: 10.1016/j.ijleo.2013.01.061
[22] NIST Atomic Spectra Database [Electronic source]. URL: https://www.nist.gov/pml/atomic-spectra-database
[23] J. Han, M.C. Heaven, G.D. Hager, G.B. Venus, L.B. Glebov. Proc. SPIE, **8962**, 896202 (2014). DOI: 10.1117/12.2045164
[24] P.A. Mikheyev, J. Han, A. Clark, C. Sanderson, M.C. Heaven. J. Phys. D, **50** (48), 485203 (2017). DOI: 10.1088/1361-6463/aa91bf
[25] A.K. Chernyshov, P.A. Mikheyev, N.I. Ufimtsev. J. Quant. Spectrosc. Rad. Transf., **222**, 84 (2019). DOI: 10.1016/j.jqsrt.2018.10.010
[26] D.J. Emmons, D.E. Weeks. J. Appl. Phys., **121** (20), 203301 (2017). DOI: 10.1063/1.4983678

Translated by D.Safin